CORE
Metadata, citation and similar papers at core.ac.uk
Provided by e-Prints Soton

Characteristics of Q-Switched Cladding-Pumped Ytterbium-Doped Fiber Lasers with Different High-Energy Fiber Designs

Cyril C. Renaud, H. L. Offerhaus, J. A. Alvarez-Chavez, J. Nilsson, W. A. Clarkson, P. W. Turner, D. J. Richardson, and A. B. Grudinin

***Abstract*—We theoretically and experimentally analyze Q-switched cladding pumped ytterbium-doped fiber lasers designed for high pulse energies. We compare the extractable energy from two high-energy fiber designs: 1) single- or few-moded low-NA large mode area (LMA) fibers and 2) large-core multimode fibers, which may incorporate a fiber taper for brightness enhancement. Our results show that the pulse energy is proportional to the effective core area and, therefore, LMA fibers and multimode fibers of comparable core size give comparable results. However, the energy storage in multimode fibers is mostly limited by strong losses due to amplified spontaneous emission (ASE) or even spurious lasing between pulses. The ASE power increases with the number of modes in a fiber. Furthermore, spurious feedback is more difficult to suppress with a higher NA, and Rayleigh back-scattering increases with higher NA, too. These effects are smaller in low-NA LMA fibers, allowing for somewhat higher energy storage. For the LMA fibers, we found that facet damage was a more severe restriction than ASE losses or spurious lasing. With a modified laser cavity, we could avoid facet damage in the LMA fiber, and reached output pulse energies as high as 2.3 mJ, limited by ASE. Theoretical estimates suggest that output pulse energies around 10 mJ are feasible with a larger core fiber, while maintaining a good beam quality.**

***Index Terms*—Double-cladding, fiber laser, large core fiber, Q-switched laser, Ytterbium.**

I. Introduction

RARE-EARTH doped fiber lasers offer an excellent combination of high efficiency and high spatial beam quality. In the high-power regime, cladding pumped fiber lasers have emerged as very efficient sources of continuous wave (CW) and pulsed radiation [1]–[4]. The combination of multi-millijoule pulse energies, peak powers around 10 kW, and a compact cavity arrangement without the need for active cooling [3] make fiber lasers an attractive alternative to comparable solid state laser for pulsed laser applications, such as nonlinear frequency conversion, range finding, and remote sensing. In contrast to conventional solid-state lasers, double-clad fiber lasers require very long cavity lengths (typically several tens of meters) to achieve efficient absorption of pump radiation from high power diode bars. The reason for this is the small core area, which leads to a large cladding-to-core area ratio and low pump absorption in typical double-clad fiber designs. The small core area with a tight mode confinement also leads to a high gain for a relatively small amount of energy stored in the gain medium in the form of excited Yb-ions. The high gain leads to losses via amplified spontaneous emission or even spurious lasing between pulses. This limits the energy that can be stored in the gain medium and thus the pulse energy of a Q-switched fiber laser. Furthermore, a long fiber and small core area exacerbate nonlinear effects like self phase modulation, stimulated Raman scattering, and stimulated Brillouin scattering. These can also be detrimental for Q-switched operation. To increase the energy storage and reduce fiber nonlinearities, it is necessary to increase the core area, which decreases the mode confinement and permits the use of shorter fibers without compromising the absorption efficiency. However, this route also leads to a multi-moded core and compromised beam quality, unless special fiber designs are used. One possibility is to use a large mode area (LMA) fiber with a complex, low-NA, refractive index profile. LMA fibers are either single- or few-moded, with selective Yb doping that also promotes high beam quality. We have recently reported a Q-switched fiber laser capable of generating 2.3-mJ pulses in a cladding-pumped configuration [3] based on LMA fiber. The core area, in this case, was 1300 μm^2, more than a factor of 50 greater than that in standard Yb-doped single-mode fibers [5]. We have also reported CW laser operation of multimode fibers with a tapered section for suppression of higher order modes [6]. This is another relatively simple possibility for a fiber laser with high beam quality and a large effective mode area with performance that can be comparable to that of LMA fibers, and is therefore attractive also for Q-switching.

In this paper, we compare the performance of Yb-doped Q-switched fiber lasers based on these two fiber types and investigate key design issues for the generation of high-energy Q-switched pulses. We first use a theoretical model to highlight the impact of core diameter and amplified spontaneous emission (ASE) on the output pulse energy. We then present experimental results for these two types of Q-switched Yb-doped fiber lasers, and compare the pulse energies to those obtained with a single-mode fiber with a normal core area.

II. Theory

The saturation energy E_{sat} is a key parameter for the amount of energy that can be stored in a laser. It is given by

$$E_{\mathrm{sat}} = \frac{h\nu_s A}{(\sigma_{es} + \sigma_{as}) \cdot \Gamma_s} \tag{1}$$

Manuscript received May 15, 2000; revised October 9, 2000.

The authors are with the Optoelectronics Research Centre, University of Southampton, Southampton SO17 1BJ, U.K. (e-mail: ccr@orc.soton.ac.uk).

Publisher Item Identifier S 0018-9197(01)00883-1.

0018–9197/01$10.00 © 2001 IEEE

Authorized licensed use limited to: UNIVERSITY OF SOUTHAMPTON. Downloaded on July 1, 2009 at 10:01 from IEEE Xplore. Restrictions apply.

where

- $h\nu_s$ signal photon energy;
- σ_{es}, σ_{as} emission and absorption cross-section at the emission wavelength (we will use the values $\sigma_{es} = 2.0 \times 10^{-20}\ \mathrm{cm}^2$, $\sigma_{as} = 1.4 \times 10^{-23}\ \mathrm{cm}^2$, which are typical values at the typical signal wavelength of 1080 nm);
- A doped area;
- Γ_s signal overlap with the active dopant.

To be more precise, this parameter can be linked to the gain the stored energy (E_{stored}) and the extractable energy (E_{ext}), using the following steps:

$$G_{\mathrm{dB}} = \frac{10}{\ln(10)}\Gamma_s\left((\sigma_{es}+\sigma_{as})\int_0^l n_2(z)\,dz - \sigma_{as}n_{\mathrm{tot}}L\right) \tag{2}$$

$$E_{\mathrm{stored}} = h\nu_s A\int_0^l n_2(z)\,dz \tag{3}$$

where n_2 and n_{tot} are the upper and total population densities (ion/m^3). Energy can only be extracted if there is a net gain in the fiber, i.e., as long as the stored energy exceeds a bleaching level E_{bleach} for which $G = 0$ dB. Thus, the extractable energy is given by

$$E_{\mathrm{ext}} = E_{\mathrm{stored}} - E_{\mathrm{bleach}}. \tag{4}$$

From (2). and (3), it follows that

$$G_{\mathrm{dB}} = \frac{10}{\ln(10)}\cdot\left(\frac{E_{\mathrm{stored}}}{E_{\mathrm{sat}}} - \frac{E_{\mathrm{bleach}}}{E_{\mathrm{sat}}}\right) = \frac{10}{\ln(10)}\cdot\frac{E_{ext}}{E_{\mathrm{sat}}} \tag{5}$$

$$E_{\mathrm{bleach}} = \sigma_{as}n_{\mathrm{tot}}\Gamma_s L\cdot E_{\mathrm{sat}}. \tag{6}$$

As a rule of thumb, the extractable energy stored in a fiber (i.e., energy above the bleaching level of the fiber) is limited to around ten times the saturation energy. Above that, any additional pumping power is simply lost as ASE between pulses, without significantly increasing the stored energy: The gain grows by $10/\ln(10) = 4.34$ dB if the stored energy increases by E_{sat}, and the energy loss to ASE by roughly the same amount, or even more in the presence of spurious feedback. Thus, the ASE power losses grow exponentially with the stored energy. Once ASE loss begins to dominate the overall power losses, further pumping soon becomes quite inefficient. Since σ_{es} and σ_{as} are more or less fixed by the dopant, the doped area A and the signal overlap Γ_s are the only parameters available for increasing the limit of storage via an increased value of E_{sat}. Note, however, that for a given refractive index geometry, A and Γ_s are not independent. Rather, the signal overlap increases with the doped area, and the ratio A/Γ_s can only be varied over a limited range if the dopant is restricted to the core (with a fixed refractive index geometry). Thus, a larger doped area does not lead to significantly larger saturation energy. Instead, special geometries like ring-doping [7] are better for increasing the ratio A/Γ_s and thus E_{sat} within a fixed refractive index geometry. Alternatively, by increasing the mode size with a modified refractive index geometry, we can also increase the ratio A/Γ_s, and this is the approach we take for a larger saturation energy in this paper.

It is also possible to change the lasing wavelength to one with smaller cross-sections to increase the saturation energy of the signal. However, it is the ASE that limits the energy storage, so the saturation energy of the ASE is what really matters. Also, the peak wavelength of the ASE can be shifted to one with a higher saturation energy (typically by increasing the fiber length in the case of a quasifour-level transition like in Yb). In practice, we found that the ASE peak did not shift significantly with fiber length for the lasers we investigated. Furthermore, in a free-running fiber laser with significant reflection in the pump launch end, the peak wavelength of the ASE can be expected to coincide with the gain peak and, therefore, with the lasing wavelength, as was, indeed, the case with our lasers.

Though the saturation energy given by the simple expression in (1) is very closely related to the maximum extractable energy from a fiber laser, other more complex, and less transparent, equations are needed for precise evaluations of the extractable energy under specific pumping conditions. Several rate equation models have been developed for the dynamics of solid-state Q-switched lasers [8]–[14]. Many of these models neglect the ASE energy loss mechanism, but for Q-switched fiber lasers, it is essential to include [15], [16]. Here, we are mainly interested in the maximum energy that can be stored and extracted at repetition rates low enough for the system to reach a steady state between pulses. A time-independent analysis of the system, including ASE, between pulses is then sufficient. We use a simple model with a single wavelength for the ASE and signal, similar to the one described in [14]

$$\frac{dP_p(z)}{dz} = -\Gamma_p\sigma_{ap}n_1(z)P_p(z) \tag{7}$$

$$\pm\frac{dP^{\pm}_{\mathrm{ASE}}(z)}{dz} = \Gamma_s(\sigma_{es}n_2(z) - \sigma_{as}n_1(z))P^{\pm}_{\mathrm{ASE}}(z) + \Gamma_s n_2(z)\sigma_{es}\cdot 2n_m h\nu_{\mathrm{ASE}}\Delta\nu_{\mathrm{ASE}} \tag{8}$$

$$n_2(z) = n_{\mathrm{tot}}\cdot\frac{\frac{P_p(z)\sigma_{ap}\Gamma_p}{h\nu_p A} + \frac{P^{\mathrm{tot}}_{\mathrm{ASE}}(z)\sigma_{as}\Gamma_s}{h\nu_{\mathrm{ASE}}A}}{\frac{P_p(z)\sigma_{ap}\Gamma_p}{h\nu_p A} + \frac{1}{\tau_2} + \frac{P^{\mathrm{tot}}_{\mathrm{ASE}}(z)(\sigma_{as}+\sigma_{es})\Gamma_s}{h\nu_{\mathrm{ASE}}A}} \tag{9}$$

$$n_1(z) = n_{\mathrm{tot}} - n_2(z) \tag{10}$$

$$P^{\mathrm{tot}}_{\mathrm{ASE}}(z) = P^{+}_{\mathrm{ASE}}(z) + P^{-}_{\mathrm{ASE}}(z). \tag{11}$$

Here, n_2 and n_1 are the upper and lower level population densities (ion/m^3), P_p is the pump power (the pumping is uni-directional), $P^{\pm}_{\mathrm{ASE}}$ is the signal power, co- (+) and counter-propagating (−) relative to the pump, $\Delta\nu_{\mathrm{ASE}}$ is the ASE bandwidth, n_m the number of transverse modes excited in the cavity (excluding polarization degeneracy), τ_2 is the lifetime of the upper laser level, and $\Gamma_{p,s}$ are the pump and signal overlaps with the doped area. The last term in equation (8) represents the spontaneous emission that seeds the ASE, considering the same ap-

Authorized licensed use limited to: UNIVERSITY OF SOUTHAMPTON. Downloaded on July 1, 2009 at 10:01 from IEEE Xplore. Restrictions apply.

proximation as in [14] for coupling of spontaneous emission into guided core modes. Rayleigh back-scattering is neglected.

In this model, we assume that the pump is evenly distributed throughout the core and inner cladding, in each transverse cross-section of the fiber, despite the fact that the inner cladding is highly multi-moded for the pump. While each mode experiences a different characteristic absorption, a practical, well-designed cladding-pumped fiber should exhibit essentially uniform absorption along its length due to a combination of mode scrambling techniques and special geometrical fiber designs. In practice, a single equation (7) is then enough to describe the evolution of all pump modes. The signal may be multi-moded as well, with different gain for different modes. In (8), we assume an effective number n_m of signal modes that see essentially the same gain. The core may support more modes than that, but we assume that the gain of those modes is low enough to neglect them. The effective number of transverse modes depends on the overlap between different modes and the gain medium as well as on how different modes saturate the gain medium.

The system of equations (7)–(11) is repeatedly integrated along the fiber until a solution is found that satisfies the boundary conditions for the ASE and pump power. For a fiber with a perpendicular cleave at the pump-launch end (with ∼4% reflectivity) and an angle cleave at the other, the boundary conditions for the pump are given by the power launched through the perpendicular fiber end. For the signal, they become

$$P_s^+(0) = 0.04P_s^-(0) \tag{12}$$

and

$$P_s^-(l) = 0 \tag{13}$$

where l is the fiber length. The solution provides the steady-state ASE power evolution and Yb inversion profile along the fiber. The extractable energy is readily evaluated as the difference between the stored energy and the energy required to bleach the Yb signal reabsorption

$$E_{ext} = h\nu_s A\left\{\int_0^l n_2(z)dz - n_{\rm tot}L\frac{\sigma_{as}}{\sigma_{as}+\sigma_{es}}\right\}. \tag{14}$$

Fig. 1 shows the extractable energy in the limit of low repetition rates as a function of pump power, calculated with the model above. The fibers had a simple step-index distribution with core diameters of 40 μm and 6 μm (Γ_s =0.75 for both). The fibers were 10-m long. The pump absorption was 3 dB/m for cladding pumping (the Ytterbium concentration was 3000 p.p.m by weight). We assumed that for both fibers the generated laser beam was single-moded, even though the large-core fiber would actually be intrinsically multi-moded. In order to demonstrate the impact of the ASE, we have also calculated the extractable energy in the absence of the ASE source term for the same fibers. The two points on the graph represent two experimental results obtained at 500 Hz, 1.3 mJ (33 μm core), and 2.3 mJ (40-μm core). This repetition rate was low enough to correspond to the regime described by our model. The two experimental points are 3-dB below the theoretical value. Background losses, which we neglected, and incomplete energy extraction are possible reasons for the discrepancy. Furthermore, the experimental conditions do not correspond exactly to the assumptions in the simulations. For example, the core size of one fiber is slightly smaller. However, at this level of absorbed pump power (5 W), ASE self-saturation is small for these core dimensions, so the results should be comparable. We conclude that the extractable energy that we calculate with our model gives a fair indication of the resulting pulse energy at low repetition rates.

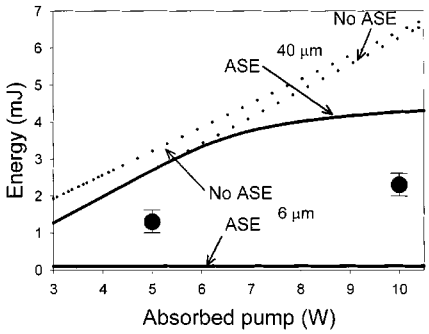

Fig. 1. Calculated extractable energy versus absorbed pump power for fibers with 6- and 40-μm diameter cores. Solid curves: ASE included in the calculations. Dashed curves: ASE suppressed in the calculations. The dots represent measured pulse energies for a 33-μm core fiber (at 5 W of absorbed pump power) and a 40-μm core fiber (at 10 W of absorbed pump power).

In Fig. 1, the calculated energy scales almost proportionally with the core area at high pump powers: for 10 W pump power the extractable energy is 0.11 mJ for the 6-μm core fiber and 4.3 mJ for the large core fiber (with core area approximately 40 times larger). For the large core fiber, the efficiency with which energy is stored rolls off above 6 W of pump power at ∼4 mJ of extractable energy. For the small core fiber, the energy storage efficiency starts to roll off already at 300 mW, and the extractable energy is limited to ∼0.1 mJ. Above these pump levels, ASE self-saturation prevents further energy storage, and a larger mode area is required to relax the ASE limit, as previously discussed. The calculations, thus, show that: 1) ASE limits energy storage at high pump powers and 2) the energy that can be stored at high pump powers is proportional to the mode area with this simple core design.

The spontaneous emission that seeds the ASE is proportional to the number of operating modes in (8). Therefore, all else being equal, a SM fiber can reach a higher gain, extractable energy, and actual pulse energy than can a MM fiber (note that even a single, typically fundamental, mode can extract all of the extractable energy from the fiber, insofar as the mode interacts with the whole doped region). Consider, for instance, a fiber laser operating on 50 transverse modes. The ASE source term is then 50 times stronger than for a SM fiber. Therefore, the gain can be 50 times (i.e., 17 dB) larger with a single mode than with 50 modes before ASE self-saturation sets in. Since the ASE is strongly seeded by the 4% reflection in one cavity end, the 17 dB is actually a double-passed gain. Thus, we expect the single-pass gain difference between a single-moded and a 50-moded fiber to be ∼8.5 dB. This gain corresponds to a stored energy of $2\times E_{\rm sat}$, or around 20%–30% of the expected extractable energy. Simulations confirmed this result.

If we keep the core of the NA fixed and increase the core diameter, the reduction in the energy storage because of increasing

Authorized licensed use limited to: UNIVERSITY OF SOUTHAMPTON. Downloaded on July 1, 2009 at 10:01 from IEEE Xplore. Restrictions apply.

ASE losses to an increasing number of modes is very much smaller than the growth of energy storage because of a larger core size. Under these premises, the area of a 50-moded core is approximately 50 times larger than that of a single-moded core. The $\sim$20% reduction of energy storage because of the extra ASE losses in a multi-mode core is negligible compared to the 50-fold increase of energy storage from the larger area. Thus, we expect the extractable energy to scale with the mode area even if the fiber becomes multi-moded.

III. Experimental Setup

The experimental setup used for the Q-switched fiber lasers is shown in Fig. 2. The fibers were end-pumped by a beam-shaped diode bar [17], delivering 35 W of power at 915 nm. Of this power, up to 25 W could be launched into a 200-μm diameter fiber. A dichroic mirror was used to separate the signal and pump at the pump launch end, which also served as the out-coupling end. The fiber was cleaved perpendicularly, and the 4% Fresnel reflection provided the feedback at this end of the cavity. The other fiber end was angle-cleaved to suppress feedback, and an external highly reflecting mirror closed the cavity. The mirror reflected back the first-order beam from an acousto-optic modulator (AOM) that was on–off modulated to act as a Q-switch. The diffraction efficiency was up to 70%, depending on beam parameters.

For measuring the pulse energy, we used a silicon detector with a time constant of $\sim$10 μs. The detector integrates the output signal over this time, so for significantly shorter pulses, the peak output signal from the detector is proportional to the pulse energy. At the same time, the integration time is sufficiently short to ensure that the signal level between pulses, generated by ASE, is negligible compared to the peak signal level from the detector (corresponding to the pulse energy). The energy detector was calibrated with the laser operating at a high repetition rate, where ASE between pulses is negligible (verified with an optical spectrum analyzer). The pulse energy is then simply the average power divided by the pulse repetition rate. The pulse energy is thus readily evaluated, and the energy detector can be calibrated accordingly. For measuring pulse shapes, we used a fast silicon detector with a time constant of less than 10 ns. For measuring average power, we used a thermal power meter.

IV. Fibers

We have investigated three types of fibers: LMA (fiber #1 and #2), multi-mode large core (MMLC, fiber #3 and #4), and single-mode fiber (#5) with a typical core geometry and NA (i.e., not designed for high energy storage). Fiber #4 was the same as fiber #3, except that the fiber was adiabatically tapered down at the pump end to single-mode core dimensions. This tapered section suppressed higher order modes in the cavity [18]. Previous work has shown that reducing the fiber diameter with a taper significantly improves the beam quality (M^2 value reduced from 2.6 to 1.4) with a low-output power penalty (1 dB) [6]. This intensity enhancement is caused by the fiber taper and the resulting selective mode excitation at the pump launch end of the laser cavity. As a rough estimation, we can take $(M^2)^2$ as an upper limit for the effective number of lasing modes. The NA of the taper (surrounded by air) is high enough to guide the pump through the taper without radiation losses, even though the fiber is significantly thinner in the taper. However, this particular taper was somewhat sharp, and incurred a pump loss of 20%.

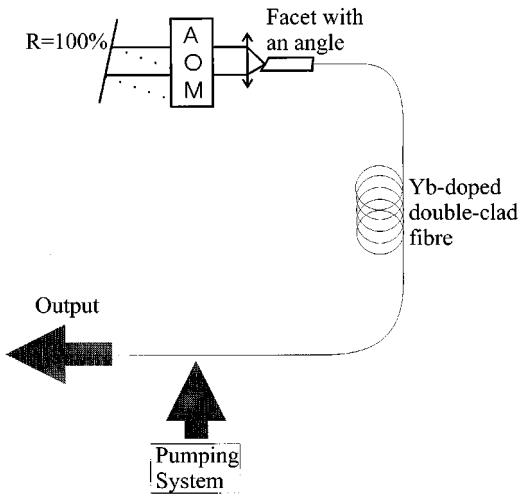

Fig. 2. Experimental setup.

The fibers were first characterized in CW operation using a setup similar to the one in Fig. 2, but without the AOM and the HR mirror. Instead, the fibers were perpendicularly cleaved at both ends, and the double-ended laser output power was measured. Table I lists important characteristics of the fiber lasers. We will primarily treat the fibers designed for high-energy storage (1–4), while fiber #5 is included for comparison.

The fibers were circular, except for fiber #2, which had a rectangular inner cladding. All fibers had a centered core. The slope efficiencies of all fibers, except #5, were approximately the same. Fiber #5 suffered from excess pump-propagation losses (about 2 dB over the length of the fiber). This reduced its slope efficiency. The pump absorption depends on the Yb concentration and the relative sizes of the doped area and the cladding area. However, it also depends on how the pump light is distributed in the cladding. Table I lists Yb concentrations calculated from the measured Yb absorption under the assumption that the pump light is evenly distributed in the inner cladding and core in each transverse cross-section of the fiber. This is not entirely correct, and the actual Yb-concentration is therefore higher than what is listed in Table I. While the M^2-value of the MMLC fiber #3 is intrinsically larger than that of the LMA fibers, a comparably low value can be obtained with a taper (fiber #4). Besides the core design, the cladding size is another important geometrical characteristic as it influences the pump-launch efficiency and, therefore, the maximum achievable output power.

V. Results and Discussion

Fig. 3 shows the pulse energy and average output power, including ASE, as a function of the repetition rate when the high-energy fibers (1–4) were Q-switched. The fibers were 10-m long, which was enough for efficient pump absorption.

Authorized licensed use limited to: UNIVERSITY OF SOUTHAMPTON. Downloaded on July 1, 2009 at 10:01 from IEEE Xplore. Restrictions apply.

TABLE I
CHARACTERISTICS OF THE FIBERS USED IN THE EXPERIMENTS

	Fiber #1	Fiber #2	Fiber #3	Fiber #4	Fiber #5
Type	LMA	LMA	MMLC	MMLC (fiber #3) with taper	SM
Core diameter [μm]	20	40	33	33	4
Dopant [$*10^{25}$ ions/m^3]	4.32	1.83	4.23	4.23	48
Cladding diameter [μm]	150	100 x 300	200	200	100
NA	0.06	0.06	0.13	0.13	0.10
M^2	1.3	3.0	7.0	1.8	1.0
CW slope efficiency with respect to absorbed pump power	70%	70%	84%	84%	50%
Pump absorption @ 915 nm [dB/m]	2.0	2.5	3.0	3.0	2.0

The pump level was adjusted to generate 3 W of laser output power with the AOM constantly on, with the setup in Fig. 2. At high repetition rates (over around 15 kHz), the average power is maintained around 3 W, and the pulse energy is simply this power divided by the repetition rate. The pulse energy grows as the repetition rate decreases and exceeds 0.5 mJ at 4 kHz for all the high-energy fibers. The average power, on the other hand, drops for low repetition rates (below 10–15 kHz), as is typical for Q-switched lasers.

Comparing the behavior of the different high-energy fibers, we see that the average power and the pulse energy from fiber #1 are smaller than that of the other fibers. The reason for this is its smaller core diameter with concomitantly smaller saturation energy. As the repetition rate is reduced, more energy is stored in the fibers between pulses. Especially for fiber #1, this leads to a large gain, which via ASE losses prevents further efficient energy storage. Most of the ASE is emitted in the AOM end of the fiber rather than in the outcoupling end. Therefore, also the average output power, including ASE and measured from the outcoupling end, drops with lower repetition rates. Fibers #2 and #3 have larger cores with larger saturation energies, and are, therefore, less influenced by this effect. Fiber #4 is the same as fiber #3, except that it includes a mode-selecting taper and emits a nearly diffraction-limited beam, while the beam from fiber laser #3 is highly multi-moded. At high repetition rates, the pulse energy is the same, as a result of the adjustment of the pump power to equal CW output power—the pumping of fiber #3 is slightly stronger to compensate for the CW signal and pump loss of the taper. However, at low repetition rates, the pulse energy depends only weakly on the pump power, because of ASE self-saturation. Thus, the stronger pumping of fiber #3 will not compensate the taper signal losses at low repetition rates. Therefore, the pulse energy and average output power become lower with fiber #4 than with #3 at low repetition rates. However, the loss in the taper is small, and the energy penalty is limited to 10%. Note also that with a better taper, losses would be even smaller. In fact, since fiber #4 operates on fewer modes than fiber #3 (see the M^2-values in Table I), ASE losses should be smaller, and fiber #4 could even generate higher-energy pulses than fiber #3 in the low repetition rate regime. However, this effect is small and more than offset by signal losses in the taper.

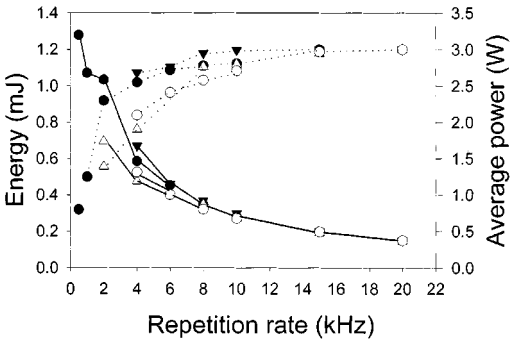

Fig. 3. Energy (solid curves) and average power (dotted curves) versus repetition rate for fiber #1 (empty triangle), fiber #2 (filled triangle), fiber #3 (filled circle), and fiber #4 (empty circle). The pump level was adjusted to generate 3 W of laser output power with the AOM constantly on.

In Fig. 3, we studied the fiber lasers over repetition rates for which we could obtain reliable Q-switching. Fiber facet damage and spurious lasing for MM fibers limited the repetition rates at low frequency, as the pulses reached peak powers exceeding the damage threshold for too low a repetition rate. This limit varied between 0.5 and 4 kHz from fiber to fiber, depending on core area and pulse duration. At high repetition rates, the pump power was not enough to re-pump the fiber between pulses, leading to missing pulses, and limiting the repetition rate upwards. The upper limit varied from fiber to fiber, too, from 10 to 20 kHz, because of differences in energy extraction efficiency as well as laser threshold, pump power, and pump intensity.

We also tried fiber #5 (with a single-mode core of standard geometry) in this configuration. The standard fiber (#5) was 5-m long with 0.8 W of CW output power with the AOM constantly on. At higher pump levels than that, it was difficult to achieve stable Q-switching. We reached a pulse energy of 70 μJ at 10-kHz repetition rate. For lower repetition rates than this, spurious lasing occurred between pulses. We conclude that with this fiber laser, a relatively small extractable energy of approximately 70 μJ already generated enough gain for lasing even with the AOM off. Compared to fiber #5, the high-energy fibers are significantly better and all relatively similar to each other, as expected given the core sizes of the different fibers.

Authorized licensed use limited to: UNIVERSITY OF SOUTHAMPTON. Downloaded on July 1, 2009 at 10:01 from IEEE Xplore. Restrictions apply.

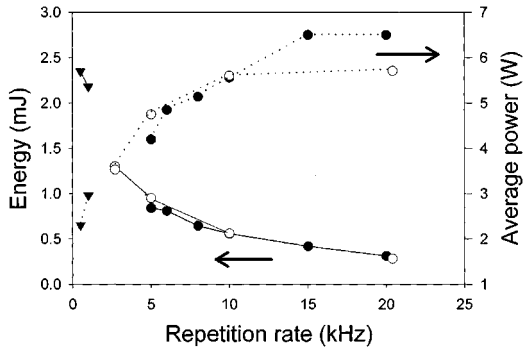

Fig. 4. Pulse energy (solid lines) and average power (dotted lines) versus repetition rate for fiber #2 (empty circle and triangle) and fiber #3 (filled circle) at maximum pump level.

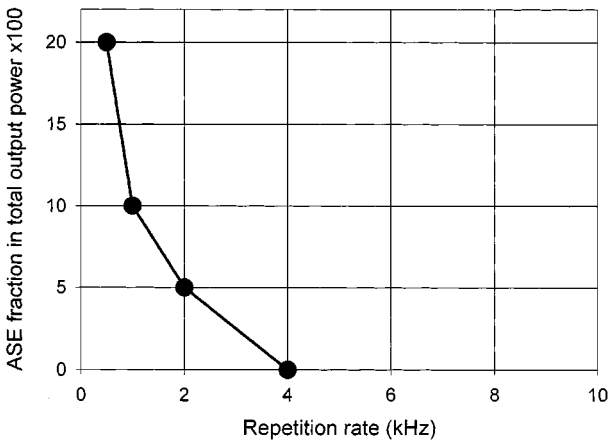

Fig. 5. Fraction of ASE in the total average power output power versus repetition rate for 10-m long pieces of fibers #2 and #3. The pump power was adjusted to generate 3 W of average power at high repetition rates. The ASE was negligible for repetition rates above 4 kHz.

The fiber lasers were then pumped ffwith maximum pump power available (35-W incident) in order to reach highest possible pulse energies and investigate pulse energy limits in this regime. We found that either damage to the facet or the onset of lasing between pulses limited the pulse energy. Damage to the out-coupling facet was observed with all fibers, at peak powers of 10–14 kW, for ~100-ns pulses (power densities in the region of 2 GW/cm^2). Onset of lasing between pulses was also observed, but only with the standard NA fibers (#3–#5). Lasing between pulses is a result of spurious feedback or Rayleigh back-scattering [19]. Both of these effects are more severe in higher-NA fibers. The amount of Rayleigh backscattering is proportional to the NA squared and to the fiber length. We estimate that Rayleigh back-scattering in the MMLC fibers is 5–10 dB stronger than in the LMA fibers, creating an effective feedback of around −30 dB. Other sources of feedback, e.g., from an imperfectly angled fiber end, are also larger with a higher NA, although these are very difficult to estimate without measurements. Fig. 4 shows pulse energy and average output power (including ASE) versus repetition rate for fibers #2 and #3. From 35 W of power from the beam-shaped diode bars, we could launch 22 W into fiber #3 and 20 W into fiber #2. For both fibers, the AOM diffraction efficiency dropped to 50%, which explains the relatively low average power now obtained. The drop in diffraction efficiency may be an effect of a degraded beam quality: at higher pump power, the fiber gain reaches a higher value, so that even higher order modes can build up to significant energy. This degrades the beam quality, which may lead to a reduced diffraction efficiency. The fibers were used in different lengths and with different setups. For fiber #2, a length of 10 m was used in the setup shown in Fig. 2 (empty circles in Fig. 4). This configuration was limited in pulse energy by facet damage. For fiber #3, a length of 10 m was used in the setup of Fig. 2 (filled circles in Fig. 4). This configuration, with a higher-NA fiber, was limited in pulse energy by spurious lasing between pulses. We also investigated a 35-m long piece of fiber #2 in a setup that included wavelength selective ASE feedback in the output-coupling end [3] (for all other Q-switched laser measurements, we used the setup of Fig. 2). With this arrangement, we reached our highest pulse energy, 2.3 mJ at 500 Hz (filled triangles in Fig. 4). The NA was sufficiently low to keep back-scattering at acceptable levels even at this fiber length. Moreover, the long fiber produced pulses that were long enough (with low enough peak powers) to prevent fiber facet damage even at the highest pulse energies.

Because reflections in the out-coupling end seeds the ASE propagating toward the AOM, most of the power lost as ASE between pulses is emitted in the AOM end. However, some ASE is also present in the laser output. This ASE typically peaks around 1040 nm. Fig. 5 shows the fraction of ASE in the laser output power for fibers #2 and #3 as a function of the repetition rate, for 10 m long fibers. The pump power was adjusted to generate 3 W of average power at high repetition rates. The ASE build-up time was about 0.4 ms for both fibers. Therefore, for both fibers, the ASE becomes significant only at pulse repetition rates below 2 kHz. The ASE reaches a level of 20% of the total power at 0.5 kHz. However, this ASE background can be reduced by using wavelength selective output coupling and ASE recycling as in [3].

For fiber #1, the ASE build-up time was 0.3 ms, with the pump power adjusted to generate 3 W of average power at high repetition rates. Thus, as expected, the gain builds up more quickly in this smaller core fiber than in fibers #2 and #3. We also measured the ASE build-up time in fiber #5. Even though the pump power was now much smaller (less than 2 W), the ASE still built up in 50 μs. This clearly demonstrates the faster ASE and gain build-up in a smaller-core fiber. Because of the fast build-up of gain in these fibers, spurious inter-pulse lasing occurred for repetition rates below 2 and 10 kHz for fiber #1 and #5, respectively. The relatively high NA with more Rayleigh back-scattering also contributes to the spurious lasing of fiber #5.

The energy of the Q-switched pulses did not depend critically on fiber length, provided that the peak power was low enough to avoid facet damage. The main influence of the length was on the temporal shape of the output pulses, as shown in Fig. 6. For this measurement, we used fiber #2 with lengths of 5, 10, 15 (not shown) and 35 m at a repetition rate of 2 kHz. The full-width half-maximum pulse durations were 80, 100, 120, and 500 ns for these fiber lengths, respectively. Measurements with 5 and 10 m of fibers #1 and #3 gave similar results. For laser cavities so long that the pulse roundtrip time exceeded the pulse dura-

Authorized licensed use limited to: UNIVERSITY OF SOUTHAMPTON. Downloaded on July 1, 2009 at 10:01 from IEEE Xplore. Restrictions apply.

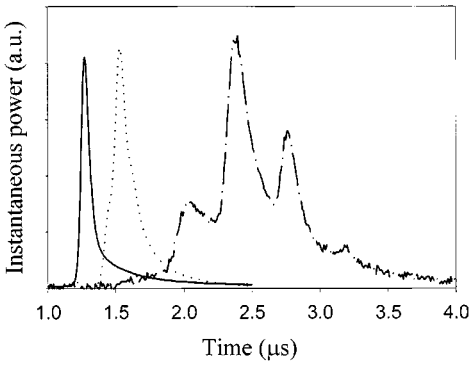

Fig. 6. Output pulse shapes from fiber #2 for different fiber lengths: 5 m (solid), 10 m (dotted), and 35 m (chain dashed). The peak powers are scaled to approximately the same value while actually, the energy (the area under the curves) is similar for the three pulses.

tion, the pulse split up as can be seen in Fig. 6 for the 35-m long fiber. Compared to short fibers, the peak intensity is then significantly reduced and the damage limitation on the fiber facet is relaxed so that a higher energy level can be reached. However, in many applications a clean single pulse is required, in which case the maximum fiber length is around 25–30 m in this case. The repletion rate influences the pulse duration, too; at higher repetition rates, the pulses become longer as the smaller amount of energy stored between pulses leads to a lower gain and a slower pulse build-up. For instance, at a repetition rate of 20 kHz, the pulse duration was between 400 and 900 ns depending on the fiber length, the pump level and the core size.

VI. Conclusion

We have theoretically and experimentally studied Q-switched cladding-pumped Yb-doped fiber lasers operating at millijoule levels. Theoretical results show that the energy storage is limited by strong ASE between pulses, because of the high gain in the fiber. Due to the tight modal confinement in fibers, the high gain appears at a relatively low energy. However, the energy storage scales with the core area. Experimentally, we have studied two types of large core fibers: low NA, few moded large mode area fibers as well as standard NA multimode fibers. For similar core sizes and at a fixed repetition rate, the energy extracted from both types of fiber was comparable, and in fair agreement with simulations. Good spatial quality was obtained directly from the LMA fiber and also from a multimode fiber incorporating a mode-selecting tapered section. We found that experimentally, although strong ASE ultimately limits the pulse energy, it was difficult to reach this limit. Instead, spurious lasing between pulses or often even fiber facet damage restricted the pulse energy. We showed that facet damage could be avoided with longer fibers, which produce longer pulses with lower peak powers. Alternatively, we believe that facet damage can be avoided with an improved fiber termination.

Compared to large-core multi-mode fibers, the complex low NA LMA design allows for higher gain before Rayleigh scattering and spurious feedback initiates lasing. They also generate less ASE at a given level of gain. Therefore, somewhat more energy can be stored at low repetition rates. With a long low-NA LMA fiber, we managed to avoid both facet damage and spurious lasing. We then reached a record pulse energy of 2.3 mJ, corresponding to the ASE limit of this fiber laser. On the other hand, multimode fibers are easier to manufacture, and the use of a simple fiber taper results in a beam quality comparable to that of the LMA fiber. Although not studied here, tapering can be used for improving the beam quality of LMA fibers, too. For example, calculations show that a fiber with a 70 μm core can reach over 20 mJ of extractable energy for pump powers exceeding 30 W. Realistically, accounting for losses and incomplete energy extraction, such a fiber should be capable of generating 10-mJ pulses. We expect that a combination of an LMA fiber and a taper would generate a high brightness beam even with a 70-μm core. Special attention should also be paid to the laser cavity design and the reduction of facet damage, e.g., by enlarging the beam diameter at the fiber facet with a taper.

References

[1] *Product Catalogs of Polaroid, Inc.*, IRE-Polus, SDL, 1999.
[2] V. Dominic, S. MacCormack, R. Waarts, S. Sanders, S. Bicknese, R. Dohle, E. Wolak, P. S. Yeh, and E. Zucker, "110 W fiber laser," *Electron. Lett.*, vol. 35, pp. 1158–1160, 1999.
[3] H. L. Offerhaus, J. A. Alvarez-Chavez, J. Nilsson, P. W. Turner, W. A. Clarkson, and D. J. Richardson, "Multi-mJ, multi-watt Q-switched fiber laser," *Opt. Lett.*, vol. 25, pp. 37–39, 2000.
[4] C. C. Renaud, R. J. Selvas-Aguilar, J. Nilsson, P. W. Turner, and A. B. Grudinin, "Compact, high energy Q-switched cladding pumped fiber laser with a tuning range over 40 nm," *IEEE Photon. Technol. Lett.*, vol. 11, pp. 976–978, 1999.
[5] N. G. R. Broderick, H. L. Offerhaus, D. J. Richardson, R. A. Sammut, J. Caplen, and L. Dong, "Large mode area fibers for high power applications," *Opt. Fiber Technol.*, vol. 5, pp. 185–196, 1999.
[6] J. A. Alvarez-Chavez, A. B. Grudinin, J. Nilsson, P. W. Turner, and W. A. Clarkson, "Mode selection in high power cladding pumped fiber lasers with tapered section," in *Conf. Lasers and Electro-Optics, OSA Technical Digest*. Washington, DC: Optical Society of America, 1999, pp. 247–248.
[7] J. Nilsson, R. Paschotta, J. E. Caplen, and D. C. Hanna, "Yb^{3+}-ring-doped fiber for high energy pulse amplification," *Opt. Lett.*, vol. 22, pp. 1092–1094, 1997.
[8] A. E. Siegman, *Lasers*. Mill Valley, CA: Univ. Sci. Books, 1986, ch. 26.
[9] Koechner, *Solid-State Laser Engineering*. Berlin, Germany: Springer-Verlag, 1996, vol. 1, ch. 8.
[10] W. L. Barnes, "Q-switched fiber lasers," in *Rare Earth Doped Fiber Lasers and Amplifiers*, M. J. F. Digonnet, Ed. New York, NY: Marcel Dekker, 1993.
[11] P. Roy and D. Pagnoux, "Analysis and optimization of a Q-switched erbium doped fiber laser working with a short rise time modulator," *Opt. Fiber Technol.*, vol. 2, pp. 235–240, 1996.
[12] I. Kelson and A. Hardy, "Strongly pumped fiber lasers," *IEEE J. Quantum Electron.*, vol. 34, pp. 1570–1577, 1998.
[13] I. Kelson and A. Hardy, "Optimization of strongly pumped fiber lasers," *J. Lightwave Technol.*, vol. 17, pp. 891–897, 1999.
[14] E. Desurvire, *Erbium-Doped Fiber Amplifiers*. New York, NY: Wiley-Interscience, 1994, ch. 1.
[15] O. G. Okhotnikov and J. R. Salcedo, "Emission buildup in Q-switched fiber lasers," *Opt. Lett.*, vol. 20, pp. 887–888, 1995.
[16] J. Nilsson and B. Jaskorzynska, "Modeling and optimization of low repetition-rate high-energy pulse amplification in cw-pumped erbium-doped fiber amplifiers," *Opt. Lett.*, vol. 18, pp. 2099–2101, 1993.
[17] W. A. Clarkson and D. C. Hanna, "Two-mirror beam-shaping technique for high-power diode bars," *Opt. Lett.*, vol. 21, pp. 375–377, 1996.
[18] M. E. Fermann, "Single-mode excitation of multimode fibers with ultrashort pulses," *Opt. Lett.*, vol. 23, pp. 52–54, 1998.
[19] R. Oron and A. A. Hardy, "Rayleigh backscattering and amplified spontaneous emission in high-power ytterbium fiber amplifiers," *J. Opt. Soc. Am. B*, vol. 16, pp. 695–701, 1999.

Authorized licensed use limited to: UNIVERSITY OF SOUTHAMPTON. Downloaded on July 1, 2009 at 10:01 from IEEE Xplore. Restrictions apply.

Cyril C. Renaud was born in Paris, France, in 1973. He received the degree of engineering from the Ecole Supˆrieure d'Optique, Orsay, France, and the DiplŸome d'Etudes Approfondies (D.E.A.) in optics and photonics from the University Paris XI, Orsay, France, in 1996.

He spent one year as engineer with Sfim-ODS, working on microchips lasers. He is currently a Research Student in the Optoelectronics Research Centre, University of Southampton, Southampton, U.K. His research field is high power Yb-doped fiber lasers, with particular interest on Q-switched system and 980-nm generation.

H. L. Offerhaus was born in Leiden, The Netherlands, in 1968. He graduated from Delft University of Technology, The Netherlands, in applied physics in 1993, and received the Ph.D. degree in high-power lasers in 1997 from the Twente University of Technology, The Netherlands.

He then spent two years at the Optoelectronics Research Centre, University of Southampton, Southampton, U.K., working on high-power fiber lasers and nonlinear optics. Currently, he is involved in high harmonic generation in gasses, clusters, and droplets at the FOM Institute of Atomic and Molecular Physics, Amsterdam, The Netherlands.

J. A. Alvarez-Chaves received the B.Eng. degree in electronics and the M.Sc. degree in telecommunications. He is currently working toward the Ph.D. degree, which involves studies in cladding-pumped Nd, Yb, and Er/Yb-doped fibre lasers and amplifiers.

He then worked for IUSACELL-Bell Atlantic before joining the Optoelectronics Research Centre, University of Southampton, Southampton, U.K., in 1997. He is a Research Student in the High-Power Fibre Lasers Group at the Optoelectronics Research Centre, University of Southampton, Southampton, U.K.

J. Nilsson, photograph and biography not available at the time of publication.

W. A. Clarkson, photograph and biography not available at the time of publication.

P. W. Turner, photograph and biography not available at the time of publication.

D. J. Richardson, photograph and biography not available at the time of publication.

A. B. Grundinin, photograph and biography not available at the time of publication.

Authorized licensed use limited to: UNIVERSITY OF SOUTHAMPTON. Downloaded on July 1, 2009 at 10:01 from IEEE Xplore. Restrictions apply.